

# P4.38 AN AEROSOL-DEPENDENT ALGORITHM FOR REMOTELY SENSED SEA SURFACE TEMPERATURES FROM THE NOAA AVHRR

Nicholas R. Nalli\*

CIRA, Colorado State University, Fort Collins, Colorado

Larry L. Stowe

NOAA/NESDIS/ORA, Washington, D.C.

## 1. INTRODUCTION

For two decades, global measurements of sea surface temperature (SST) have been produced by the National Oceanic and Atmospheric Administration (NOAA) using infrared (IR) data obtained from the Advanced Very High Resolution Radiometer (AVHRR) on board NOAA polar orbiting satellites (Walton *et al.*, 1998). The conventional retrieval algorithms provide a multichannel correction for IR attenuation due to molecular water vapor absorption under non-cloudy conditions. However for atmospheric conditions with anomalously high aerosol content (e.g., arising from dust, haze, biomass burning and volcanic eruptions), such algorithms lead to significant negative biases in SST due to unaccounted attenuation arising from aerosol absorption and scattering.

The standard multichannel SST (MCSST) relies on an observed quasi-linear statistical relationship between spectral window brightness temperatures and *in situ* measurements of “bulk” surface temperature obtained by oceanographic buoys (Walton *et al.*, 1998). Because of the nonlinear dependence of transmission on total absorber amount for the global range of water vapor, a nonlinear SST (NLSST) algorithm has also been implemented. However, it is difficult to separate the spectral signal caused by atmospheric aerosols from that caused by water vapor using only 2–3 channels in the IR. Although the empirical coefficients can account for the attenuation in a mean sense, they cannot account for anomalous aerosol loading. Hence the MCSST and NLSST equations lead to significant negative biases (i.e.,  $\overline{T'_S} - T_S < 0$ , where  $T'_S$  and  $T_S$  are the retrieved and “true” SST, respectively) under such conditions without additional information.

This paper overviews a simple aerosol correction for AVHRR SST using measurements of visible solar reflectance at 0.63 and 0.83  $\mu\text{m}$  in AVHRR channels

1 and 2, respectively (after Nalli and Stowe, 2001). A unique, globally comprehensive (both spatially and temporally) AVHRR matchup data sample is employed that includes retrievals of channel 1 aerosol optical depth (AOD). It is then empirically shown that the SST bias caused aerosols can be expressed as a parametric equation in two variables, these being the observed AVHRR channel 1 slant-path AOD, and the ratio of channels 1 and 2 normalized albedos. Based on these relationships, aerosol correction equations are derived for the daytime multichannel and nonlinear SST (MCSST and NLSST) algorithms. Separate sets of coefficients are utilized for two aerosol modes: Tropospheric (e.g., dust, smoke, haze) and Stratospheric/Tropospheric (e.g., following a major volcanic eruption). The elimination of cold biases in the AVHRR SST will greatly improve its utility for the general user community and in climate research.

## 2. DATA

Data used in our empirical analyses originate from the AVHRR Pathfinder Program, a collaborative effort led by NOAA and the National Aeronautics and Space Administration (NASA). Specifically, the AVHRR Pathfinder Atmospheres (PATMOS) and Oceans Pathfinder Matchup Database (PFMDB) data sets are merged to provide a unique PATMOS matchup data base. The two Pathfinder data sets are briefly described below.

### 2.1 Pathfinder Atmospheres (PATMOS)

PATMOS is a retrospective data set consisting of re-processed AVHRR 5-channel data mapped to a quasi-equal area grid (110 km)<sup>2</sup> over the time period spanning 1981–2000 (Stowe *et al.*, 2001). These data include the grid-cell means and standard deviations of AVHRR channels 1 and 2 (0.63 and 0.83  $\mu\text{m}$ ) normalized albedos, channels 3–5 (3.7, 11, 12  $\mu\text{m}$ ) radiances, and channel 1 AOD,  $\tau_a$ , obtained from the 2nd Generation retrieval algorithm (Stowe *et al.*,

---

\* Corresponding author address: Dr. Nicholas R. Nalli, Cooperative Institute for Research in the Atmosphere (CIRA), NOAA/NESDIS E/RA1, Washington, DC 20233, USA; e-mail: nick.nalli@noaa.gov

1997). The Clouds from AVHRR (CLAVR-1) cloud mask (Stowe *et al.*, 1999) is employed to obtain clear-sky statistics. Global observations were obtained under conditions of tropospheric haze, dust and smoke outflows from continents, as well as during the entire residence time of the Mt. Pinatubo (1991–93) stratospheric aerosol layer.

## 2.2 Pathfinder Matchup Database (PFMDB)

PFMDB is maintained on the internet by the NASA Jet Propulsion Laboratory (Kilpatrick *et al.*, 2001). It consists of global *in situ* observations taken by moored and drifting buoys that have been matched-up in space and time with AVHRR overpasses spanning 1985–1998. Of particular importance are the measurements of bulk surface temperatures,  $T_b$ , taken at depths on the order of 1 m. The matchup database also provides ancillary data used in our research, namely the NCEP Reynolds OISST extracted from the filtered weekly field.

## 3. METHOD

The magnitude of aerosol-induced attenuation in the IR will depend a number of factors, the more important ones being (1) the IR optical depth, (2) the effective temperature of the absorbing layer and (3) the particle size distribution. The latter of these provides information the relative proportions of extinction resulting from absorption and scattering. Assuming there is a correlation between AOD in the visible and IR, the channel 1 AOD can provide information about the first factor. However absorber temperature and particle size cannot be objectively inferred from AOD alone.

To put a constraint on the absorber temperature, it is necessary to first characterize the integrated aerosol content as belonging to one of two modes: Tropospheric and Stratospheric/Tropospheric (or Strato/Trop for short). This is to distinguish the difference in IR attenuation expected from absorbing layers confined to a relatively warm planetary boundary layer versus those found in the colder stratosphere after a major volcanic eruption.

Because the particle size distribution within either aerosol mode can exhibit considerable variation over time and space, the IR attenuation can also show variations independent of the AOD. Previous researchers (e.g., Haggerty *et al.*, 1990; May *et al.*, 1992) have suggested that the ratio of normalized reflectance measurements between channels 1 and 2,  $R_1/R_2$ , is sensitive to the particle size distribution. We therefore propose 2 predictors for modeling the SST depression

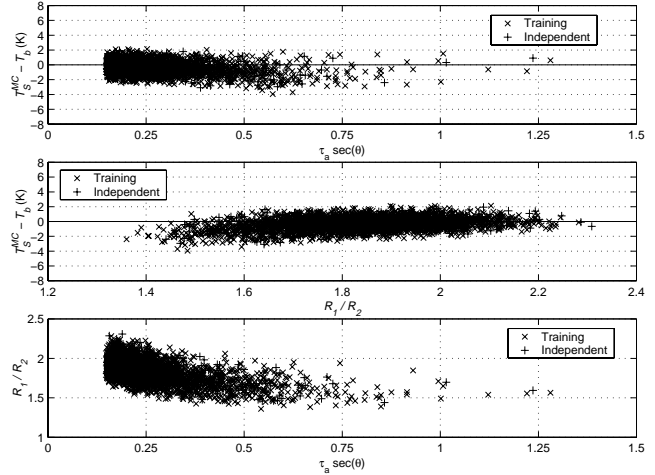


Figure 1: Regression parameter relationships, Tropospheric Mode: (top)  $\delta T_S$  and  $x_1$ , (middle)  $\delta T_S$  and  $x_2$  and (bottom)  $x_2$  and  $x_1$ . The training and independent data sets used for regression and validation are distinguished from one another using different symbols.

due to anomalous aerosol loading  $\delta T_S \equiv T'_S - T_S$ :

$$x_1 \equiv \tau_a \sec(\theta), \quad (1)$$

$$x_2 \equiv R_1/R_2, \quad (2)$$

where parameters are given by the spatial mean values from PATMOS matchup grid-cells.

Because coefficients for operational SST algorithms are determined under background tropospheric aerosol conditions, it is necessary to estimate an AOD threshold for delineating background conditions from elevated levels. The PATMOS AOD background thresholds are taken to be  $\tau_0^{\text{tropo}} = 0.15$  and  $\tau_0^{\text{strato}} = 0.10$  for the Tropospheric and Strato/Trop Modes, respectively.

## 4. STATISTICAL ANALYSIS

For the Tropospheric Mode, NOAA-14 data are taken from the years 1995–1998. For the Strato/Trop Mode, NOAA-11 data are taken during the Mt. Pinatubo residence time period of July 1, 1991 through 1992. Figures 1 and 2 show that the standard MC-SST equation, derived under background aerosol conditions ( $\tau_a < 0.15$ ), does not account for the attenuation caused by aerosols. For a given aerosol mode, the most simple model for the SST depression,  $\delta T_S = T_S - T_b$ , would be merely be a linear equation in  $x_1$

$$\delta T_{S1} = a_0 + a_1 x_1. \quad (3)$$

May *et al.* (1992) first demonstrated this relationship using a small sample of drifting buoy matchup data ob-

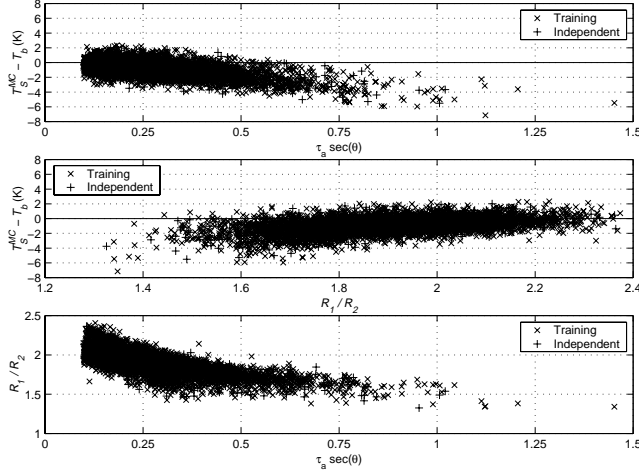


Figure 2: Same as Figure 1 except for the Strato/Trop Mode.

tained off the coast of Africa from mid-June through September, 1990. To help account for tropospheric variations in aerosol particle size, we incorporate the albedo ratio predictor,  $x_2$ , allowing 3 potential expressions (linear, interaction and full quadratic) for the response surface  $\delta T_S$  in  $x_1, x_2$  space. These are written as

$$\delta T_{S2} = a_0 + a_1 x_1 + a_2 x_2, \quad (4)$$

$$\delta T_{S3} = a_0 + a_1 x_1 + a_2 x_2 + a_{12} x_1 x_2, \quad (5)$$

$$\delta T_{S4} = a_0 + a_1 x_1 + a_2 x_2 + a_{12} x_1 x_2 + a_{11} x_1^2 + a_{22} x_2^2. \quad (6)$$

The coefficients  $a_i$  and  $a_{ij}$  are derived using a training data subset (approximately 4/5) taken randomly from the quality controlled data samples. The remaining 1/5 of data are then reserved as an independent data set. The aerosol-corrected SST is then simply given by

$$T_S = T'_S - \delta T_S, \quad (7)$$

where  $T'_S$  can be given by either the MCSST or NLSST, and  $\delta T_S$  is calculated using any one of equations (3)–(6).

## 5. VALIDATION

To validate the regression models, independent data samples from both aerosol modes are used. Results using model equation (6) as an aerosol correction for the NLSST are displayed in Figures 3 and 4 for Tropospheric and Strato/Trop Modes, respectively.

The top panels in these figures show scatterplots of  $\delta T_S$  versus buoy SST obtained from the NLSST equation, along with the aerosol corrected value (ANLSST)

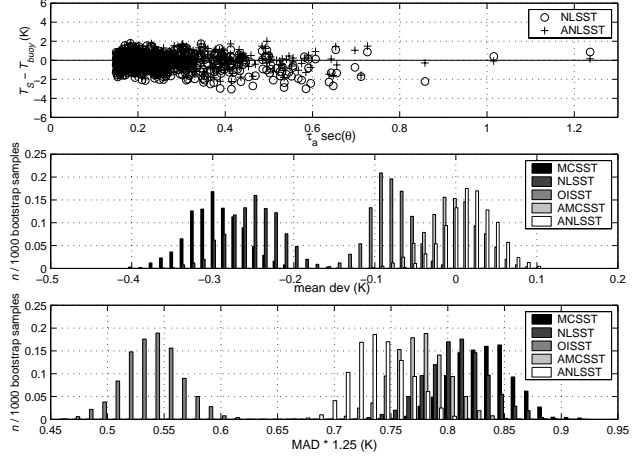


Figure 3: Aerosol corrected NLSST (ANLSST) statistics for Tropospheric aerosol mode, independent data set ( $n = 612$ ): (top) scatterplot of retrieved NLSST and ANLSST minus buoy SST, (middle) statistical bootstrap histogram of bias error, and (bottom) scatter about the mean. For reference, bootstrap histograms of the NCEP Reynolds OISST are also shown.

obtained by subtracting equation (6). These plots demonstrate the ability of the quadratic algorithm to correct for aerosol attenuation under the global range of slant path AOD under both aerosol modes. Using the linear equation (3) yields very similar results on the Strato/Trop mode, but leads to significant positive bias for the Tropospheric mode at slant path AOD  $\gtrsim 0.55$  as described above.

The middle and bottom panels of Figures 3 and 4 provide a statistical inference of the bias (mean deviation) and scatter (mean absolute deviation, MAD, scaled by a factor of 1.25) expected from the different SST algorithms using the Efron bootstrap method (i.e., random resampling with replacement). Results are shown for the standard MCSST and NLSST, the NCEP Reynolds OISST as given in the PFMDB, and the aerosol corrected MCSST and NLSST (AMCSST and ANLSST) using equation (6). Observable in the MCSST and NLSST are significant negative biases (middle panels) ranging from  $[-0.35, -0.20]$  and  $[-1.0, -0.85]$  for the Tropospheric and Strato/Trop Modes, respectively. The NCEP Reynolds OISST reduces the bias to within  $[-0.12, -0.05]$  and  $[-0.20, -0.10]$ . The aerosol dependent equations, however, yield the best results, with bootstrap histograms nearly centered about zero for both modes. The aerosol corrected results also exhibit less scatter than the uncorrected as seen in the bottom panel. The reason the PATMOS derived SSTs show higher scatter than the NCEP Reynolds

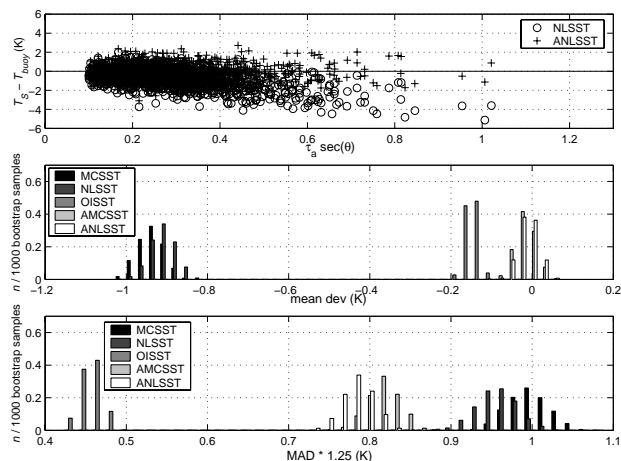


Figure 4: Same as Figure 3 except for the Strato/Trop aerosol mode ( $n = 1092$ ).

OISST is because of precision loss in the IR channel brightness temperatures (Nalli and Stowe, 2001) and not because of the algorithm.

## 6. CONCLUSION AND FUTURE WORK

This research demonstrates empirically that AVHRR observations of normalized visible reflectance in channels 1 and 2 can be utilized to provide a correction for IR attenuation from elevated aerosol levels which otherwise lead to negative biases in remotely sensed sea surface temperature (SST). The Phase I daytime algorithms will be implemented for real-time and retrospective retrievals, including a PATMOS-based SST climatology. Subsequently, in Phase II, the 3rd Generation 2-channel AVHRR AOD retrieval will be used to better model the tropospheric aerosol correction under varying aerosol types and particle sizes.

## ACKNOWLEDGEMENTS

This project is funded by the NESDIS Ocean Remote Sensing Program managed under Dr. A. Strong. We are grateful to Mr. A. Kidd, manager of the NOAA/NESDIS Satellite Active Archive, for providing access to the daily PATMOS data sets. We also thank Dr. B. Huang (UW-Madison) for informal correspondences about descriptive statistics.

## REFERENCES

Haggerty, J. A., Durkee, P. A., and Wattle, B. J. (1990). A comparison of surface and satellite-derived

aerosol measurements in the western Mediterranean. *J. Geophys. Res.*, **95**, 1547–1557.

Kilpatrick, K. A., Podestá, G. P., and Evans, R. (2001). Overview of the NOAA/NASA advanced very high resolution radiometer Pathfinder algorithm for sea surface temperature and associated matchup database. *J. Geophys. Res.*, **106**(C5), 9179–9197.

May, D. A., Stowe, L. L., Hawkins, J. D., and McClain, E. P. (1992). A correction for saharan dust effects on satellite sea surface temperature measurements. *J. Geophys. Res.*, **97**(C3), 3611–3619.

Nalli, N. R. and Stowe, L. L. (2001). Aerosol-dependent algorithms for remotely sensed sea surface temperatures from the NOAA AVHRR. *J. Atmos. Ocean. Tech.* In preparation.

Stowe, L. L., Ignatov, A. M., and Singh, R. R. (1997). Development, validation, and potential enhancements to the second-generation operational aerosol product at the National Environmental Satellite, Data and Information Service of the National Oceanic and Atmospheric Administration. *J. Geophys. Res.*, **102**(D14), 16,923–16,934.

Stowe, L. L., Davis, P. A., and McClain, E. P. (1999). Scientific basis and initial evaluation of the CLAVR-1 global clear/cloud classification algorithm for the advanced very high resolution radiometer. *J. Atmos. Ocean. Tech.*, **16**, 656–681.

Stowe, L. L., Jacobowitz, H., Ohring, G., Knapp, K., and Nalli, N. R. (2001). The advanced very high resolution radiometer Pathfinder Atmosphere (PATMOS) climate data set: Initial analyses and evaluations. *J. Climate*. Submitted May, 2001.

Walton, C. C., Pichel, W. G., Sapper, J. F., and May, D. A. (1998). The development and operational application of nonlinear algorithms for the measurement of sea surface temperatures with the NOAA polar-orbiting environmental satellites. *J. Geophys. Res.*, **103**(C12), 27,999–28,012.